A Practical Approach to Vector-acoustic Imaging of Primaries and Free-surface Multiples

WS06-C03

A Practical Approach to Vector-acoustic Imaging of Primaries and Free-surface Multiples

M. Ravasi* (University of Edinburgh), I. Vasconcelos (Schlumberger Gould Research), A. Curtis (University of Edinburgh) & A. Kritski (Statoil)

SUMMARY

Free-surface multiples travel different paths and illuminate different volumes of the subsurface than primaries. When used jointly with primaries to image the subsurface by means of forward and backward extrapolation of separated down- and up-going wave components respectively, free-surface multiples have been shown to improve the continuity of shallow parts of the subsurface image by suppressing acquisition related footprints.

We show that by carefully combining the full pressure and particle velocity data by means of newly developed, vector-acoustic boundary conditions, wavefronts can be forward and backward propagated without ambiguity in their propagation direction. Wavefield decomposition is thus naturally incorporated within the extrapolation procedure.

Moreover, ocean-bottom acquisition geometries generally present source coverage that is wider than the receiver array. A strategy is proposed to incorporate in our imaging scheme energy of primary events whose direct source illumination lies outside of the receiver aperture. This is achieved by combining a directly modelled source illumination with the recorded (down-going) data.

Introduction

Imaging in areas of complex geology calls for novel acquisition and imaging techniques that include as much as possible of the useful seismic energy recorded during acquisition. In marine seismics, free-surface related multiples are an example of such seismic energy and represent a useful form of signal for the construction of a subsurface image (Muijs et al., 2007; Whitmore et al., 2010). Including multiples in imaging can improve the illumination of the shallow subsurface where images of primaries are generally affected by the acquisition footprint due to coarse shot and/or receiver spacing (Lu et al., 2011).

If up- and down-going components of the recorded wavefield are available from data that are acquired with multi-component streamers or ocean-bottom cables, primaries and multiples can be jointly imaged by forward propagation of the down-going component and backward propagation of the up-going component (Figure 1) followed by a deconvolution imaging condition (Guitton et al., 2007). It is important to note that a necessary condition for any primary reflection to be properly imaged is that both its down- and up-going legs travel through and are recorded by the receiver array. In ocean-bottom systems the source coverage is generally wider than the receiver array, so this condition is not satisfied for all sources (Figure 1 – see red arrow).

The contribution of this work is two-fold: we show that explicit up/down separation by, e.g., PZ summation (Barr and Sanders 1989) can be avoided if pressure and vertical velocity data are combined by means of newly developed, vector-acoustic (VA) boundary conditions (Vasconcelos, 2013; Amundsen and Robertsson, 2014), which allow 'on-the-fly' separation of up- and down-going fields during their forward or backward propagation. Then we define a practical strategy to jointly image free-surface multiples and primaries, including energy from those primary events whose direct source illumination lies outside of the receiver array. Our approach is tested on a 2D line of the Volve OBC field dataset from the North Sea.

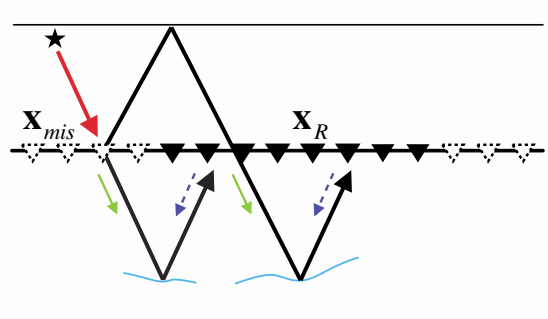

Figure 1 *A primary down-going event (red arrow) not recorded at the receiver array. This arrival needs to be numerically modelled and added to the recorded data at locations* $\boldsymbol{x}_{mis}$ *to allow consistent joint imaging of primaries and multiples by forward propagation of the down-going field (green arrows) and backward propagating the up-going field (dashed blue arrows).*

Theory of forward and backward vector-acoustic injection

Forward or backward propagation of vertical particle velocity (v_z) and pressure (p) with monopole (q) and vertical dipole (f_z) injection sources respectively, allows for separation on-the-fly into the up- and down-going components of the recorded field. An injection procedure that backpropagates up-going waves only downward and down-going waves only upward is given by (e.g., Vasconcelos, 2013)

$$\left(p^* \Rightarrow f_z\right) \& \left(-v_z^* \Rightarrow q\right) \tag{1}$$

where * refers to time-reversal (or complex conjugation in frequency domain), $\Rightarrow$ defines injection of a specific data-type (left side) with a specific source-type (right side) in the modeling code (e.g., finite-difference), and '&' is used to stress that pressure and (negative) normal particle velocity should be injected simultaneously.

Similarly, an injection procedure that forward propagates up-going waves only upward and down-going waves only downward can be achieved by injecting (e.g., Vasconcelos et al., 2014)

$$\left(p \Rightarrow f_z\right) \& \left(v_z \Rightarrow q\right) \tag{2}$$

We refer to Ravasi et al. (2014) for a description of the workflow used to apply the vector-acoustic injection scheme in equation 1 to a field dataset, and here we show a time snapshot of the forward extrapolated vector-acoustic data (Figure 2) where down-going waves (black arrows) are successfully forward propagated only below the receiver array.

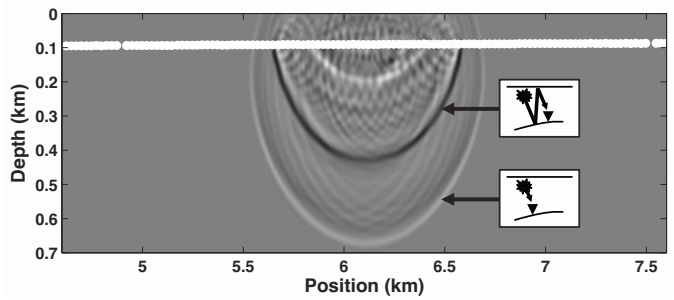

Figure 2 *Fixed-time snapshot of forward-time extrapolation. The white line denotes the location of the receiver array on the seabed where the data are injected, and the black arrows identify two down-going waves that are forward propagated only downward.*

Source wavelet calibration and augmented data

Our approach to joint imaging of primaries and free-surface multiples is composed of two parts: calibration and migration.

Initially, we find a calibration filter such that a modeled direct wave matches that in the forward propagated recorded data at a chosen depth level, rather than at the acquisition surface as in Majdanski et al. (2014). By assuming invariance of the source signature from shot to shot, this procedure is accomplished for a single shot in the center of the shot line and comprises three steps:

1. forward modeling of a generic source wavelet s (e.g., 20 Hz Ricker wavelet) from the source location to a chosen depth level z_{cal},
2. VA-forward injection (equation 2) of the recorded data to the depth level z_{cal}, and
3. extraction of the first arriving wave for both wavefields and least-squares matching.

Once a matching filter a has been estimated, this is applied to the source wavelet s and migration is performed for each shot gather as follows:

4. forward modeling of the calibrated source wavelet $s_{cal}=a\cdot s$ from any source location to the array of missing receivers $\mathbf{x}_{mis}$ and creation of an *augmented* data, the concatenation of pressure and velocity data at locations $\mathbf{x}_R$ and modelled direct arrival at locations $\mathbf{x}_{mis}$,
5. VA-forward injection of the data generated at step 4 along the augmented receiver line,
6. VA-backward injection (equation 1) of the recorded data along the receiver line, and
7. deconvolution imaging condition (Guitton et al., 2007).

Example

Volve is a small oil field in the gas/condensate-rich Sleipner area of the North Sea with a dome-shaped structure formed by the collapse of adjacent salt ridges during the Jurassic period (Szydlik et al., 2007). For this study we select a receiver line of the 3D OBC dataset containing 235 receivers with an interval of 25 m and a sail line 12 km long with a shot interval of 50 m (see Figure 4a).

The calibration procedure is illustrated in Figure 3. First, the recorded data from a shot at horizontal location x_S=6 km is injected by means of equation 2 along the receiver array and the forward propagated down-going field is recorded along a line at a chosen depth level (for example, z_{cal}=3.5 km - Figure 3a). Similarly forward modeling is carried out from the same source location using a Ricker wavelet of central frequency f_c=20 Hz (Figure 3b). Calibration of the directly modeled direct wave within the white lines in Figure 3c provides a filter that can be applied to the original Ricker wavelet (insert in Figure 3b) to create a new wavelet (insert in Figure 3c) consistent with that of the real data. Note that when the recorded data is forward propagated by means of VA injection, direct and refracted waves that generally overlap in the data propagate towards different directions. This results in a much cleaner direct wave at depth for the source wavelet calibration procedure. The calibrated wavelet is then used to generate an augmented data for each shot location as explained in step 4. Figure 3d shows a good agreement in the kinematics and dynamic of the recorded and modelled direct wave at transitions (black dashed lines) between physical receivers $\mathbf{x}_R$ and missing receivers $\mathbf{x}_{mis}$.

The augmented data is migrated as described in steps 5-7 in the smooth velocity model (Figure 4a) and the resulting image is shown in Figure 4d. For comparison we also image the up-going component of the recorded data using as input for the source wavefield both the calibrated source wavelet s_{cal} (i.e., imaging of primaries - Figure 4b) and the down-going component of the recorded data (Figure 4c). When no attempt to remove free-surface multiples from the recorded data is made, the image of primaries shows artefacts due to the incorrect handling of multiples that reach the

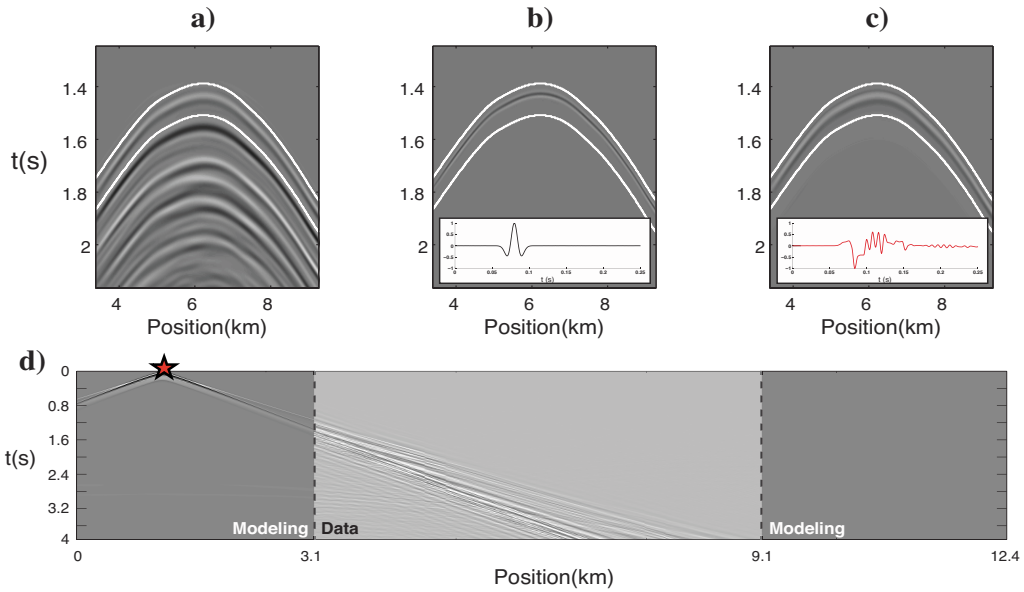

Figure 3 *Calibration procedure. Pressure field recorded at z_{cal}=3.5 km for a) forward propagated data, b) forward modelled wavelet, and c) forward modelled wavelet after calibration. Inserts in b) and c) show the original and calibrated source wavelet. d) Augmented data for a source at x_S=1 km (outside of the receiver array aperture).*

recording array as up-going fields (green arrows in Figure 4b). While imaging of primaries should only be applied after removing all free-surface multiples from the data via, e.g. up/down deconvolution, we show that including free-surface multiples in the source wavefield and applying a deconvolution imaging condition (Guitton et al., 2007; Muijs et al., 2007) could represent an alternative approach to reduce cross-talk between primaries and multiples and to attenuate the related artefacts.

Joint imaging of primaries and free-surface multiples using the augmented data provides also a noticeably wider illumination (see dashed boxes in Figure 4d) than that obtained from the recorded data alone. Note, however, that since multiples do not contribute to the image inside the areas enclosed by dashed lines boxes, cross-talk artefacts are not attenuated there (red circle in Figures 4b and 4d). With primaries providing a wider illumination of deeper geology, free-surface multiples are instead very beneficial in the shallow structure, compensating for the lack of illumination of primaries in presence of coarse shot spacing (e.g., Δx_S=500 m) as shown in Figure 5. The acquisition footprint is reduced and the continuity of the shallow structure is improved.

Conclusions

Two vector-acoustic boundary conditions have been proposed for forward and backward extrapolation of down- and up-going components of multi-component ocean-bottom data without the need for preliminary wavefield separation. A deconvolution imaging condition of these extrapolated fields allows for imaging of primaries and free-surface multiples with limited cross-talk artifacts. We have also shown that to take full advantage of the wider aperture provided by primaries, recorded data need to be combined prior to migration with a matched estimate of the first arriving down-going wave at locations where receivers are not present.

Acknowledgements

The authors are grateful to the Edinburgh Interferometry Project (EIP) sponsors (ConocoPhillips, Schlumberger Cambridge Research, Statoil and Total) for supporting this research. We would like to thank Statoil ASA and the Volve license partners ExxonMobil E&P Norway and Bayerngas Norge, for the release of the Volve data.

References

Amundsen, L, and Robertsson, J.O.A [2014] Wave equation processing using finite-difference propagators, Part 1: Wavefield dissection and imaging of marine multicomponent seismic data. Geophysics, **79**, (6), T287-T300.
Barr, F. J., and Sanders, J. I. [1989] Attenuation of water-column multiples using pressure and velocity detectors

in a water-bottom cable. 59th Annual International Meeting, SEG, Expanded Abstracts.
Guitton, A., Valenciano, A., Bevc, D., and Claerbout, J. [2007] Smoothing imaging condition for shot-profile migration. Geophysics, **72**, (3), S149-S154.
Lu, S., Whitmore, N.D., Valenciano, A.A., and Chemingui, N. [2011] Imaging of primaries and multiples with 3D SEAM synthetic. 81st SEG Annual Meeting, Expanded Abstracts, 3217-3221.
Majdanski, M., Kostov, C., Kragh, E., Moore, I., Thompson, M., & Mispel, J., 2011. Attenuation of free-surface multiples by up/down deconvolution for marine towed-streamer data, Geophysics, **76**, V129–V138.
Muijs, R., Robertsson, J. O. A., and Holliger, K. [2007] Prestack depth migration of primary and surface-related multiple reflections: Part I — Imaging. Geophysics, **72**, (2), S59–S69.
Ravasi, M., Vasconcelos, I., Curtis, A., and Kritski, A. [2014] Vector-Acoustic reverse-time migration of Volve OBC dataset without up/down decomposed wavefields. Second EAGE/SBGf Workshop 2014.
Szydlik, T., Smith, P., Way, S., Aamodt, L., and Friedrich, C. [2007] 3D pp/ps prestack depth migration on the Volve field. First Break, **25**, 43–47.
Vasconcelos, I. [2013] Source-receiver reverse-time imaging of dual-source, vector-acoustic seismic data. Geophysics, **78**, (2), WA147-WA158.
Vasconcelos, I., Ravasi, M., and van der Neut, J. [2014] An interferometry-based, subsurface-domain objective function for waveform inversion. 76th EAGE Conference & Exhibition, Extended Abstracts.
Whitmore, N.D., Valenciano, A. A., Sollner, W., and Lu, S. [2010] Imaging of primaries and multiples using a dual-sensor towed streamer. 80th Annual International Meeting, SEG, Expanded Abstract.

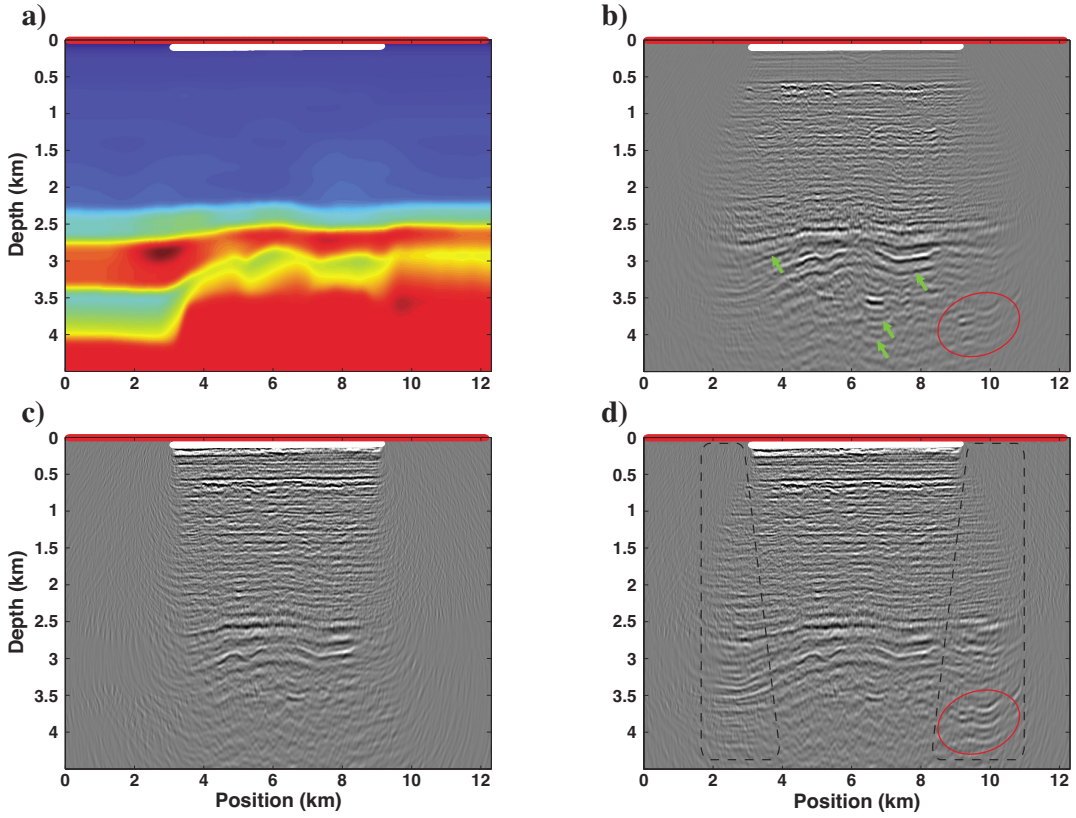

Figure 4 *a) Migration velocity model, source (red) and receiver (white) lines. b) Imaging of primaries by forward modelling of the source wavefield and VA-backward injection of the up-going data, c) imaging of primaries and multiples by VA-forward injection of the down-going recorded data and VA-backward injection of the up-going data, and d) imaging of primaries and multiples by VA-forward injection of down-going augmented data and VA-backward injection of the up-going data. Note that no attempt to suppress free-surface multiples from the recorded data is made.*

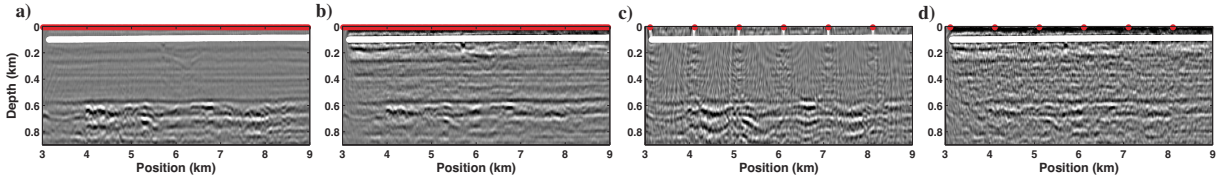

Figure 5 *Close-ups of shallow section for (a and c) imaging of primaries and (b and d) imaging of primaries and multiples by forward injection of augmented data. In c) and d) the source array has been decimated by a factor of 10 (i.e., Δx_S=500 m).*